Combined HMG-COA reductase and prenylation inhibition in treatment of CCM

Sayoko Nishimura[a,1], Ketu Mishra-Gorur[a,1], JinSeok Park[b,c], Yulia V. Surovtseva[d], Said M. Sebti[e,f], Andre Levchenko[b,c], Angeliki Louvi[a,g,2], and Murat Gunel[a,g,h,2]

[a]Department of Neurosurgery, Yale School of Medicine, New Haven, CT 06520; [b]Department of Biomedical Engineering, Yale University, New Haven, CT 06520; [c]Yale Systems Biology Institute, Yale University, West Haven, CT 06516; [d]Yale Center for Molecular Discovery, Yale University, West Haven, CT 06516; [e]Department of Drug Discovery, Chemical Biology and Molecular Medicine Program, Moffitt Cancer Center, Tampa, FL 33612; [f]Department of Oncologic Sciences, Morsani College of Medicine, University of South Florida, Tampa, FL 33612; [g]Department of Neuroscience, Program on Neurogenetics, Yale School of Medicine, New Haven, CT 06520; and [h]Department of Genetics, Yale School of Medicine, New Haven, CT 06520

Edited by Jeremy Nathans, Johns Hopkins University, Baltimore, MD, and approved April 13, 2017 (received for review February 20, 2017)

Cerebral cavernous malformations (CCMs) are common vascular anomalies that develop in the central nervous system and, more rarely, the retina. The lesions can cause headache, seizures, focal neurological deficits, and hemorrhagic stroke. Symptomatic lesions are treated according to their presentation; however, targeted pharmacological therapies that improve the outcome of CCM disease are currently lacking. We performed a high-throughput screen to identify Food and Drug Administration-approved drugs or other bioactive compounds that could effectively suppress hyperproliferation of mouse brain primary astrocytes deficient for CCM3. We demonstrate that fluvastatin, an inhibitor of 3-hydroxy-3-methylglutaryl (HMG)-CoA reductase and the *N*-bisphosphonate zoledronic acid monohydrate, an inhibitor of protein prenylation, act synergistically to reverse outcomes of CCM3 loss in cultured mouse primary astrocytes and in *Drosophila* glial cells in vivo. Further, the two drugs effectively attenuate neural and vascular deficits in chronic and acute mouse models of CCM3 loss in vivo, significantly reducing lesion burden and extending longevity. Sustained inhibition of the mevalonate pathway represents a potential pharmacological treatment option and suggests advantages of combination therapy for CCM disease.

cerebral cavernous malformations | fluvastatin | zoledronic acid | mevalonate pathway | high-throughput screen

Cerebral cavernous malformations (CCMs) are common vascular malformations that develop in the brain, spinal cord, and, more rarely, the retina (1, 2). The lesions consist of dilated sinusoidal channels lined with a single layer of endothelium devoid of vessel wall elements. CCM disease is often asymptomatic, but on occasion the lesions rupture leading to hemorrhagic stroke. Other common symptoms are headache, seizures, and focal neurological deficits. Treatment options include observation of asymptomatic lesions, antiepileptic medication, and surgical excision of lesions in patients with symptomatic or repetitive hemorrhages or intractable seizures; however pharmacological therapies that improve outcome are lacking. CCM disease is usually sporadic, although 20% of patients carry loss-of-function mutations in one of three genes: *CCM1* (also known as "*KRIT1*"), *CCM2*, and *CCM3* (also known as "*PDCD10*") (3), which encode structurally unrelated cytoplasmic proteins with critical roles in endothelial cells (4) and, uniquely for CCM3, in neurons and astrocytes as well (5, 6). CCM3 loss in neural progenitors results in hyperproliferation/activation of brain astrocytes and enhanced activity of RhoA in vivo and increased proliferation and survival of primary astrocytes in vitro (5, 6). We took advantage of these well-defined cellular phenotypes of CCM3 loss to explore potential pharmacological treatment options for CCM. High-throughput screening of available drugs identified fluvastatin, a 3-hydroxy-3-methyl-glutaryl (HMG)-CoA reductase inhibitor as a top candidate. In combination with the *N*-bisphosphonate zoledronic acid monohydrate (zoledronate), fluvastatin effectively reversed the effects of CCM3 loss in primary astrocytes and in *Drosophila* glial cells in vivo. Moreover, combined treatment with fluvastatin and zoledronate in vivo prevented neural and vascular defects and reduced lesion burden while extending lifespan in chronic and acute mouse models of CCM3. Our results suggest that combined therapy with fluvastatin and zoledronate might have therapeutic effects in CCM.

Results

Identification of Therapeutic Candidates for CCM Disease by High-Throughput Screening. To identify available medicines effective for treatment of CCM, we used high-throughput screening to search for drugs that reverse the marked increase in proliferation of CCM3-deficient ($Ccm3^{-/-}$) primary astrocytes isolated from *hGfap/Ccm3* conditional knockout (cKO) neonatal mice (5). We screened 3,806 bioactive compounds [kinase and phosphatase inhibitor sets and Food and Drug Administration (FDA)-approved drugs] using the collections at the Yale Center for Molecular Discovery (Fig. 1*A* and *SI Materials and Methods*). We identified 165 "screen-active" candidates that inhibited proliferation more than 2 SDs from the median; 54 remained for further evaluation after hit-picking, which eliminated ineffective (<50% effect) and toxic compounds. The remaining 25 hits (19 drugs because of duplications) included five statins (cerivastatin, mevastatin, fluvastatin, simvastatin, and pitavastatin), five antineoplastic drugs, six

Significance

Cerebral cavernous malformations (CCMs) are common vascular anomalies of the central nervous system that can lead to seizures, focal neurological deficits, and brain hemorrhage. Clinical options are limited mainly to treatment of symptoms or surgical resection, and targeted pharmacological therapy is lacking. Here we undertake a high-throughput screen and identify fluvastatin and zoledronate, two drugs already approved for clinical use for other indications, which act synergistically to reverse outcomes of CCM3 loss. Used in combination, fluvastatin and zoledronate effectively attenuate neural and vascular deficits in mouse models of CCM in vivo, significantly reducing formation of lesions and extending longevity. Our studies suggest that combined therapy targeting the mevalonate pathway might have therapeutic effects in CCM disease.

Author contributions: S.N., K.M.-G., J.P., A. Levchenko, A. Louvi, and M.G. designed research; S.N., K.M.-G., and J.P. performed research; Y.V.S. assisted with the high-throughput screen; S.M.S. contributed new reagents; A. Levchenko supervised research; S.N., K.M.-G., J.P., and A. Louvi analyzed data; S.N., K.M.-G., and A. Louvi wrote the paper; and A.Louvi and M.G. revised the paper.

The authors declare no conflict of interest.

This article is a PNAS Direct Submission.

Freely available online through the PNAS open access option.

[1]S.N. and K.M.-G. contributed equally to this work.

[2]To whom correspondence may be addressed. Email: angeliki.louvi@yale.edu or murat.gunel@yale.edu.

This article contains supporting information online at www.pnas.org/lookup/suppl/doi:10.1073/pnas.1702942114/-/DCSupplemental.

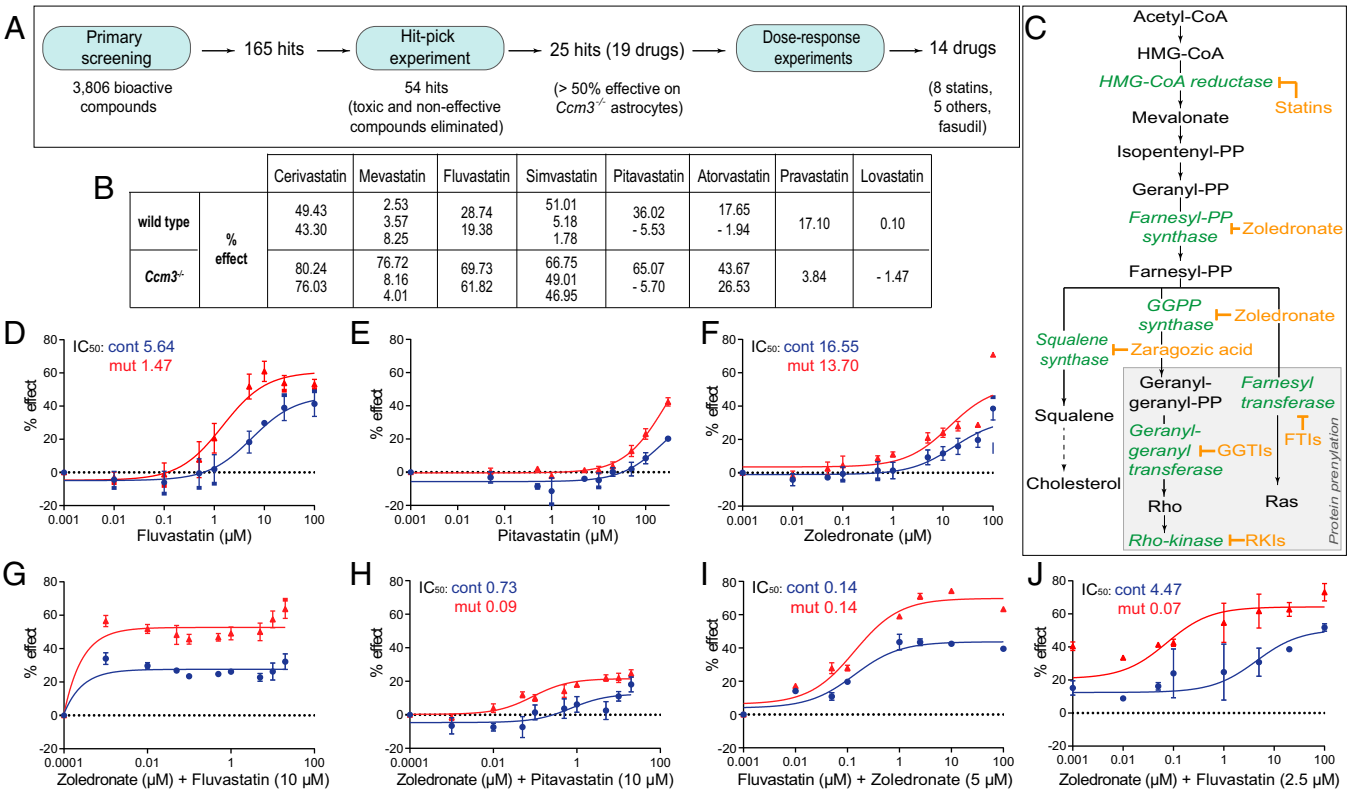

Fig. 1. The fluvastatin and zoledronate combination reverses aberrant proliferation of *Ccm3*$^{-/-}$ astrocytes. (*A*) Flowchart of the primary screening, hit-pick, and dose–response experiments. (*B*) Percent (%) effect of statins on proliferation of wild-type and *Ccm3*$^{-/-}$ astrocytes in primary screening. Some statins were present in duplicate or triplicate, as indicated by the multiple % effect values provided. (*C*) The mevalonate pathway and its branches. Statins and zoledronate respectively inhibit HMG-CoA reductase and farnesyl pyrophosphate and geranyl-geranyl pyrophosphate synthases. Additional inhibitors are indicated. (*D–H*) Dose–response curves for serial dilutions (0.001–100 μM or 0.0001–100 μM) of fluvastatin, pitavastatin, and zoledronate alone or in combination. Fluvastatin (*D*) is effective without toxic effect on wild-type cells. Pitavastatin (*E*) is mildly effective only at high concentrations; zoledronate (*F*) has no effect. (*G* and *H*) Zoledronate is more effective in combination with fluvastatin (*G*) than in combination with pitavastatin (*H*). (*I* and *J*) Dose–response curves for dilutions (0.001–100 μM) of fluvastatin and zoledronate. Zoledronate lowers the IC_{50} of fluvastatin from 1.47 to 0.14 μM (*D* and *I*); conversely, fluvastatin lowers the IC_{50} of zoledronate from 13.7 to 0.07 μM (*F* and *J*). IC_{50} values for each drug and each genotype are indicated. Results are averages of at least three paired independent experiments.

antibiotics, and three others, amounting to a hit rate of 0.657% (Fig. 1*A* and Table S1). Thus, statins (Fig. 1 *B* and *C*) represented a major drug group capable of affecting aberrant proliferation of *Ccm3*$^{-/-}$ astrocytes.

Next, we performed dose–response studies for the above hits and for atorvastatin, pravastatin, and lovastatin (which were not positive in primary screening), and the Rho kinase inhibitor fasudil hydrochloride (fasudil), despite its being approved only in Japan and China, but not in the United States or Europe, because it was shown to be effective in CCM mouse models (7, 8). Fluvastatin, cerivastatin, lovastatin, and simvastatin (Fig. 1*D* and Fig. S1 *A–C*) reversed aberrant proliferation of *Ccm3*$^{-/-}$ astrocytes, without apparent toxic effect on wild-type cells, whereas pitavastatin, mevastatin, atorvastatin, and pravastatin (Fig. 1*E* and Fig. S1 *D–F*) were only mildly effective at very high concentrations; fasudil (Fig. S1*G*) showed no effect. Other compounds were either unsuitable for CCM (the fungicide thiram and pyrithione zinc, used in the treatment of seborrheic dermatitis) or ineffective (BAY11-7082, patulin, and mitoxantrone hydrochloride) (Fig. S1 *H–L* and Table S1). They were excluded from follow-up studies, together with cerivastatin (withdrawn from the market by the FDA); simvastatin [ineffective in CCM mouse models (9–11)]; mevastatin (never marketed); and atorvastatin, pravastatin, and fasudil (all ineffective in our screen). The rather inefficient "super-statin" pitavastatin (Fig. 1*E*) was retained for further experiments as a control against fluvastatin and lovastatin, the remaining candidates after the dose–response studies.

The *N*-Bisphosphonate Zoledronic Acid Monohydrate Potentiates the Efficacy of Fluvastatin. Statins competitively inhibit HMG-CoA reductase and hence reduce cholesterol biosynthesis (Fig. 1*C*). In addition, they affect other processes that depend on the mevalonate pathway, including protein prenylation, a posttranslational modification of G proteins (12) such as RhoA, which is activated upon CCM protein loss (4). Statins normally are effective only at high doses; hence, we searched for FDA-approved drugs that could act synergistically to increase fluvastatin (or lovastatin) efficacy. Nitrogenous (N) bisphosphonates block protein prenylation by inhibiting the farnesyl pyrophosphate and geranyl-geranyl pyrophosphate synthases (Fig. 1*C*) and have synergistic effects with statins on cell lines (13) and in vivo (14). We therefore used primary astrocytes to investigate zoledronic acid monohydrate (zoledronate; not included in the primary screening), which is standard of care for patients with bone disease (15, 16) and may have antiangiogenic properties (17).

Zoledronate affected the proliferation of *Ccm3*$^{-/-}$ astrocytes at high concentrations, albeit not as efficiently as statins, whereas the nonnitrogenous bisphosphonate clodronic acid (clodronate) (18) had no effect (Fig. 1*F* and Fig. S2*A*). Therefore, we tested the efficacy of zoledronate in combination with lovastatin, fluvastatin, or pitavastatin at the dose (10 μM) used in the screen. Dose–response studies indicated that zoledronate was more effective with fluvastatin than with either pitavastatin or lovastatin (Fig. 1 *G* and *H* and Fig. S2*B*). Because 10 μM fluvastatin was very potent, we titrated zoledronate and fluvastatin to identify optimal concentrations. Dose–response studies for zoledronate with fluvastatin (Fig. 1 *I* and *J* and Fig. S2 *C–F*) or pitavastatin (control)

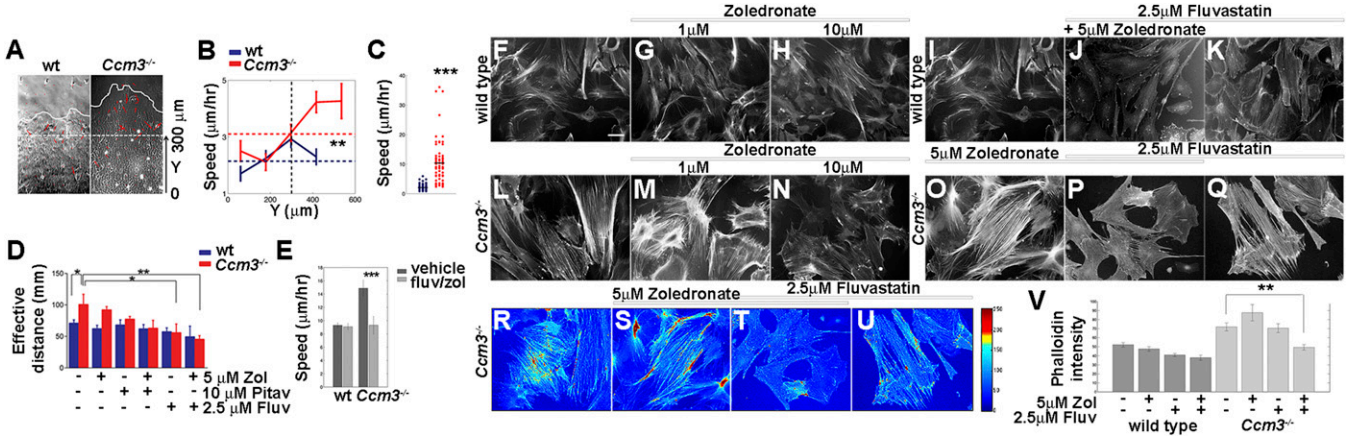

Fig. 2. Combined treatment with fluvastatin and zoledronate reduces several cellular phenotypes of *Ccm3*$^{-/-}$ primary astrocytes. (*A* and *B*) Collective migration of wild-type and *Ccm3*$^{-/-}$ astrocytes on grooved substrata. (*A*) Expansion of monolayers over a period of 48 h. The dashed and curved solid lines indicate boundaries at $t = 0$ and $t = 48$ h, respectively. Red arrows indicate the results of particle image velocity (PIV) analysis and describe the velocity of particles representing individual cells in the images. Arrow length corresponds to speed, and arrow direction indicates direction of movement. (*B*) Quantitative PIV analysis of collective cell migration. Horizontal dashed lines indicate averaged speed values; vertical dashed lines indicate the boundary of monolayers at $t = 0$. $^{**}P < 0.001$; Wilcoxon signed-rank test. (*C*) Speed of migration of individual wild-type and *Ccm3*$^{-/-}$ astrocytes on grooved substrata ($n = 60$). Horizontal lines represent averaged values for each group. $^{***}P < 0.0005$; Wilcoxon signed-rank test. (*D*) Classical scratch assay. Quantification of the effective distance migrated in the 48 h after scratching. Drugs were added 24 h before scratching. Each assay was performed in triplicate on freshly isolated primary astrocytes growing in monolayers and was repeated three times on independent preparations of wild-type and *Ccm3*$^{-/-}$ astrocytes. Results are representative of three paired independent experiments. $^{*}P < 0.05$, $^{**}P < 0.005$. (*E*) Speed of individual cell migration on grooved substrata ($n = 40$) cultured for 72 h in medium supplemented with vehicle or with fluvastatin (2.5 μM) and zoledronate (5 μM). Drug treatment suppresses the increased migration speed of *Ccm3*$^{-/-}$ astrocytes without impacting migration of wild-type counterparts. $^{***}P < 0.0005$. (*F–Q*) Representative images of wild-type (*F–K*) and *Ccm3*$^{-/-}$ (*L–Q*) primary astrocytic cultures stained with phalloidin to reveal F-actin fibers. *Ccm3*$^{-/-}$ astrocytes form stress fibers (*L*). Combined treatment reverses stress fiber formation (*P*). Primary astrocytes were cultured for 72 h in normal medium (*F*, *I*, and *L*) or in medium supplemented with zoledronate (*G*, *H*, *M*, *N*, and *O*), fluvastatin (*K* and *Q*), or both (*J* and *P*). *F* and *I* are duplicates. Results are representative of three paired independent experiments. (*R–V*) Quantitative analysis of phalloidin intensity density in primary astrocytic cultures. (*R–U*) Representative images of *Ccm3*$^{-/-}$ cultures stained with phalloidin. (*V*) Mean density of phalloidin intensity. Error bars represent SEM. $^{**}P < 0.005$. Results are averages of three paired independent experiments.

(Fig. S2 *G–J*) indicated that the zoledronate-fluvastatin combination was synergistic and effective. In *Ccm3*$^{-/-}$ astrocytes, 5 μM zoledronate effectively lowered the IC_{50} of fluvastatin from 1.47 to 0.14 μM (Fig. 1 *D* and *I*), and, conversely, 2.5 μM fluvastatin effectively lowered the IC_{50} of zoledronate from 13.7 to 0.07 μM (Fig. 1 *F* and *J*). In fact, fluvastatin at an even lower concentration (1 or 0.5 μM) effectively reduced the IC_{50} of zoledronate from 13.7 to 0.79 μM or 0.91 μM, respectively (Fig. S2 *D* and *E*).

Combined Treatment with Fluvastatin and Zoledronate Reverses the Effects of CCM3 Loss in Vitro. We then investigated the effect of combined treatment on additional outcomes of CCM3 loss. *Ccm3*$^{-/-}$ primary astrocytes migrate faster than wild-type astrocytes on grooved substrata (Fig. 2 *A–C* and Fig. S3) and in the classic scratch assay (Fig. 2*D* and Fig. S3). Combined treatment effectively attenuated migration in both assays without an obvious effect on wild-type cells (Fig. 2 *D* and *E* and Fig. S3). Moreover, treatment with fluvastatin (but not pitavastatin) and zoledronate suppressed actin stress fibers, an indicator of RhoA activation that is characteristic of *Ccm3*$^{-/-}$ astrocytes (Fig. 2 *F–V* and Fig. S4 *A–F*), resulting in diminished RhoA association with the membrane (Fig. 3*A* and Fig. S4*G*). Finally, activated astrocytes express VEGFA (19), and indeed *Ccm3*$^{-/-}$ astrocytes expressed high levels of VEGFA, which was significantly reduced by drug treatment (Fig. 3 *B* and *C* and Fig. S4*H*). Therefore, low-dose fluvastatin and zoledronate reduced the aberrant proliferation and the increased migration, stress fiber formation, and VEGFA expression associated with CCM3 loss in primary astrocytes.

Fluvastatin with Zoledronate Treatment Modulates the JNK Pathway. The drugs had no clear effect on known CCM3 interactors [the kinases MST3/STK24, MST4/MASK/STK26, or YSK1/SOK1/STK25 (20)], indicating that these are not likely to mediate drug action (Fig. S4*I*). However, fluvastatin alone or together with zoledronate inhibited both JNK1 and ERK1/2 phosphorylation, whereas the pitavastatin-zoledronate combination affected only ERK1/2 (Fig. 3 *D–G*), suggesting that fluvastatin and zoledronate specifically modulated the JNK pathway.

To dissect further the mechanism underlying the marked effect of zoledronate on the IC_{50} of fluvastatin, we tested inhibitors of mevalonate pathway branches (Fig. 1*C*). Zaragozic acid, an inhibitor of squalene synthase, had no effect (Fig. S5 *A–C*). Inhibitors of geranyl-geranyl transferase (GGTIs; namely, GGTI-298, -2417, and -286) (Fig. S5 *D–L*), Rho kinase (RKIs; RKI-1447 and fasudil) (Fig. S5 *M–R*), and farnesyl transferase (FTIs, namely, FTI-277, and -2153) (Fig. S5 *S–X*) each affected the IC_{50} of fluvastatin, but none did so as effectively as zoledronate (1–2 μM vs. 0.1–0.2 μM) (Fig. 1*I* and Fig. S5), suggesting that sustained inhibition of the main trunk of the pathway (by fluvastatin and zoledronate) is more potent than inhibition of the main trunk (by fluvastatin) and of one of its branches (by GGTIs, RKIs, or FTIs), possibly because of compensatory alternative feedback mechanisms in the latter case.

Combined Treatment Reverses Cell-Autonomous and Non–Cell-Autonomous Effects of Astrocytic CCM3 Loss in Flies and Mice in Vivo. Having established drug efficacy in primary astrocytes, we next assessed their effects in model organisms. In *Drosophila*, a genetically tractable model, the drugs attenuated glial cell proliferation in a dose-dependent manner following RNAi targeting *CG5073*, the single ortholog of *Ccm3* (21), and also inhibited the JNK and ERK pathways (Fig. S6), suggesting that *Drosophila* may be useful for rapidly testing candidate compounds.

Next, we investigated the effects of combined treatment using two mouse models of CCM3 loss. In the first model, *hGfap/Ccm3* cKO mice, the constitutive loss of CCM3 leads to hyperproliferation and activation of astrocytes and disrupts the development of the retinal vasculature (5, 6), which forms on a template of astrocytes emerging from the optic nerve (22). Fluvastatin (250 μM; 30 mg·kg^{-1}·d^{-1}) and zoledronate (500 μM; 40 mg·kg^{-1}·d^{-1})

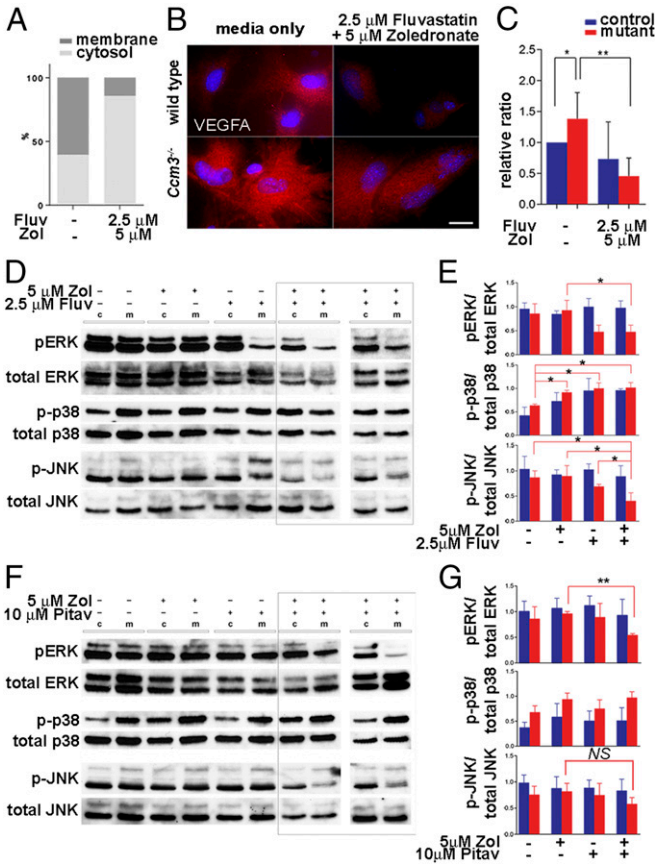

Fig. 3. Mechanistic effects of fluvastatin and zoledronate in primary astrocytes. (*A*) In *Ccm3*$^{-/-}$ astrocytes, RhoA preferentially accumulates in the membrane fraction indicating increased activation; combined treatment results in RhoA enrichment in the cytosolic fraction ($P = 0.0026$). Results are averages of three independent experiments. (*B* and *C*) *Ccm3*$^{-/-}$ astrocytes express increased VEGFA protein. (*B*) Immunofluorescence analysis indicates increased levels of VEGFA in *Ccm3*$^{-/-}$ astrocytes, which are significantly reduced by drug treatment. (*C*) Western blot analyses of cell lysates from astrocytes cultured in normal medium or in medium supplemented with drugs. Quantitative analysis indicates significant up-regulation VEGFA in *Ccm3*$^{-/-}$ astrocytes compared with wild-type astrocytes (*$P = 0.0256$). The drugs result in significant reduction of VEGFA in *Ccm3*$^{-/-}$ astrocytes (**$P = 0.0073$). Results are averages of three paired independent experiments. (*D*–*G*) Western blot (*D* and *F*) and quantitative analyses (*E* and *G*) of lysates of wild-type (control, c) and *Ccm3*$^{-/-}$ (mutant, m) astrocytes. Fluvastatin/zoledronate (*D* and *E*) inhibit activation of JNK1 and ERK1/2, but not p38, in *Ccm3*$^{-/-}$ astrocytes. Pitavastatin/zoledronate (*F* and *G*) inhibit phosphorylation of ERK1/2 but not JNK1 ($P = 0.1082$). Two independent experiments are shown for each combination (indicated by the rectangles in *D* and *F*). Results are averages of three paired independent experiments. *$P < 0.05$; **$P < 0.005$.

were administered in drinking water to pregnant dams or lactating females for 4–7 d at doses previously used in animal studies and within the range recommended for humans (23–25). In some experiments, zoledronate (100 μg·kg^{-1}·d^{-1}) was injected s.c. instead. Neonates were analyzed at P2. The drugs abrogated the increased proliferation of *Ccm3*$^{-/-}$ astrocytes in a dose-dependent manner, as assessed by the reduced levels of *Aldh1L1*, a specific marker of astrocytes (Fig. 4 *A*–*F*′ and Fig. S7 *A*–*D*) (26). Retinal endothelial cell migration onto *Ccm3*$^{-/-}$ astrocytes is increased at P2, as compared with P1 (5), and was considerably reduced by drug treatment (Fig. 4*G* and Fig. S7 *E*–*J*), which therefore reversed cell-autonomous (in astrocytes) as well as non–cell-autonomous (in retina) effects of astrocytic CCM3 loss. Finally, both delivery routes for zoledronate were effective (Fig. S7), and treatment of control littermates with the drug combination had no obvious adverse effects in vivo.

Combined Treatment Reverses Outcomes of Endothelial CCM3 Loss in Vivo and Extends Longevity. We next tested the effects of combined treatment in an endothelial cell-specific, acute model of CCM3 disease. We used inducible *Cdh5(PAC)CreERT2/Ccm3* cKO mice, which develop vascular malformations in the cerebellum and retina (27) that respond to pharmacological manipulation (28). Newborn pups were induced with tamoxifen and then were injected daily with fluvastatin [15 mg·kg^{-1}·d^{-1} intragastrically (i.g.)] and zoledronate (100 μg·kg^{-1}·d^{-1} i.p.) starting at P2. Brains and retinae were analyzed at P6. Drug treatment significantly reduced cerebellar lesion burden (Fig. 5 *A*–*F*′ and *G*–*T*) and, moreover, partially rescued retinal blood vessel dilation and vascular malformations at the periphery of the retinal vascular network (Fig. 5 *A*′′–*F*′′ and *U*). Previous work showed that KLF2/4 are up-regulated following CCM loss in endothelial cells (29–33). KLF2/4 signals were increased in the cerebellum of cKO mice, but the drugs did not reverse this effect (Fig. S8). Finally, sustained drug treatment significantly prolonged the survival of cKO mice induced with a full dose of tamoxifen at P1 or P6 (Fig. 5 *V* and *W*) and even extended the longevity of mice induced with a low dose of tamoxifen at P6 to generate a subacute CCM model (Fig. 5*X*). In conclusion, combined treatment with fluvastatin and zoledronate reversed phenotypes in mice with CCM3 loss in vivo, suggesting a potential pharmacological therapy of CCM disease that warrants further investigation. Remarkably, although the drugs were initially identified and validated in astrocytes and in a chronic model of neural CCM3 loss in vivo, they also were effective in an acute model of endothelial CCM3 loss, demonstrating efficacy in more than one cell type.

Discussion

Here, we report a potential combination therapy for CCM disease compatible with human administration. We demonstrate

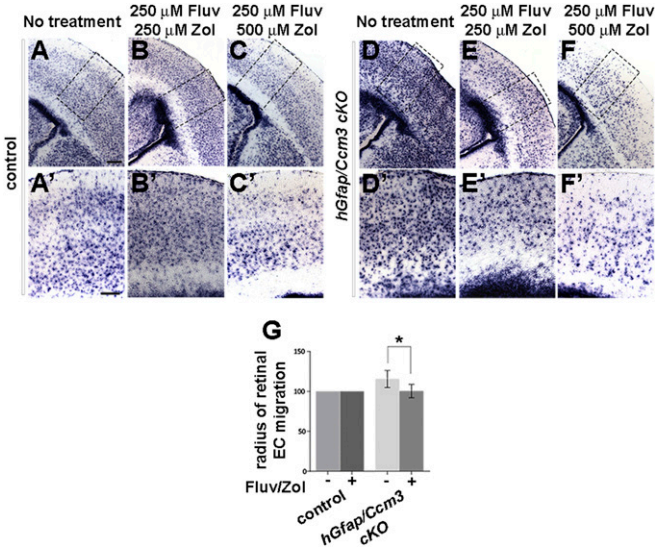

Fig. 4. Combined treatment with fluvastatin and zoledronate reverses outcomes of chronic astrocytic CCM3 loss in vivo. (*A*–*F*′) The drugs reverse astrocyte hyperproliferation in *hGfap/Ccm3* cKO brain. Representative images of coronal sections from neonates following treatment of pregnant dams or nursing females as indicated. The sections were processed for in situ hybridization with *Aldh1L1*, a marker of astrocytes. (*A*′–*F*′) Higher-magnification images of the boxed areas in *A*–*F*. (Scale bars: 0.2 mm in *A*–*F* and 0.05 mm in *A*′–*F*′.) Results are representative of eight paired independent observations. (*G*) Quantification of the radius of endothelial cell migration in flattened retinae dissected from P2 pups. The drugs decelerate migration in *hGfap/Ccm3* cKO retinae. $n = 9$ pairs of untreated and treated retinae; *$P < 0.05$.

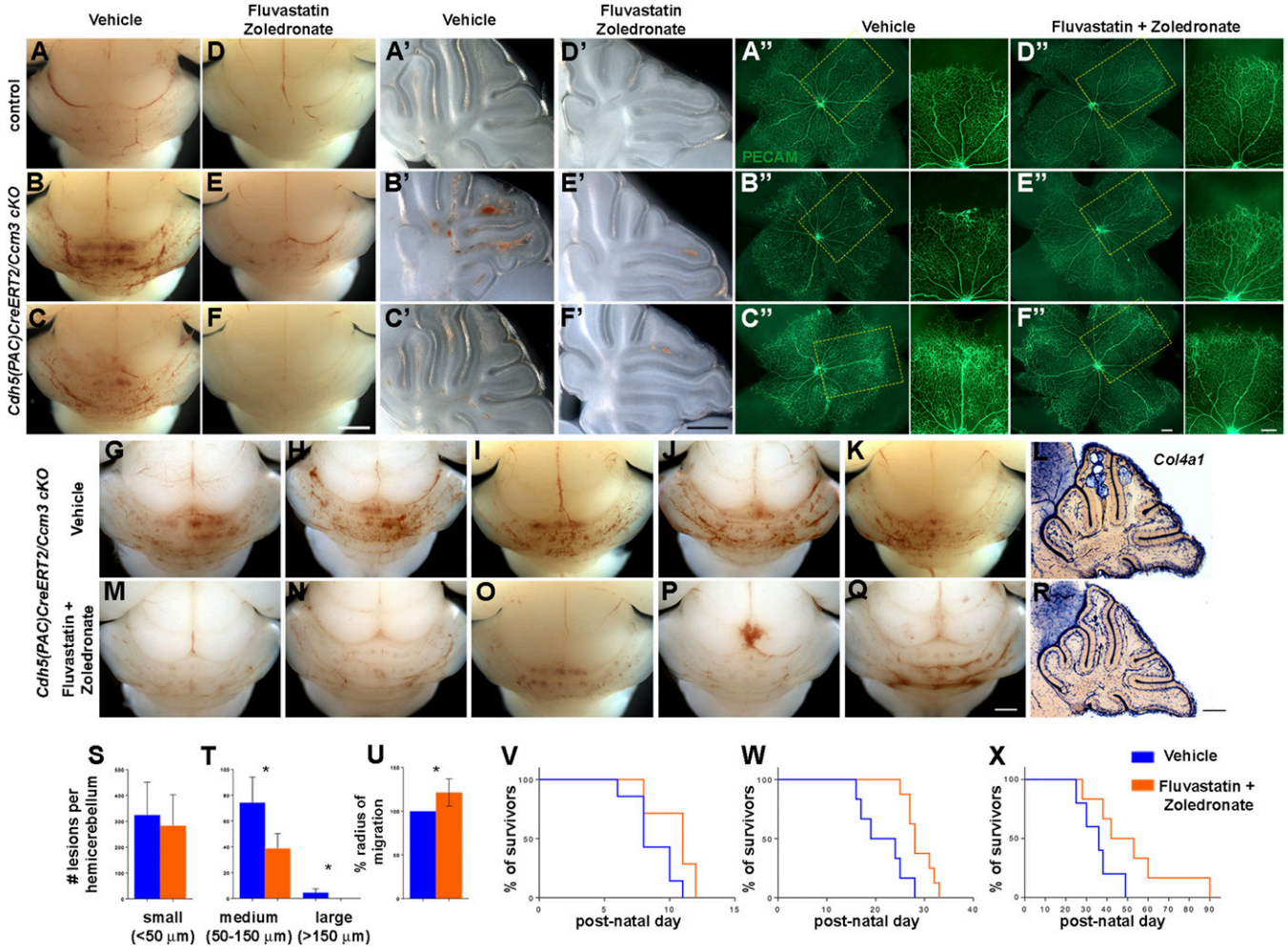

Fig. 5. Combined treatment with fluvastatin and zoledronate reverses outcomes of acute endothelial CCM3 loss in vivo. (*A–U*) The drugs decrease lesion burden (*A–F′* and *G–T*) and reverse retinal vascular defects (*A″–F″* and *U*) in *Cdh5(PAC)CreERT2/Ccm3* cKO mice. (*A–K* and *M–Q*) Whole-mount brains (*A–F*), corresponding sagittal sections through the cerebellum (*A′–F′*), and corresponding flattened retinae (*A″–F″*) from mice induced with tamoxifen at P1, injected daily with vehicle (*A–C* and *G–K*) or fluvastatin and zoledronate (*D–F* and *M–Q*), and analyzed at P6. (*A–A″* and *D–D″*: wild-type control; *B–C″*, *E–F″*, *G–K*, and *M–Q*: cKO.) Pups received daily injections of vehicle (*A–C*) or fluvastatin (i.g. 15 $mg{\cdot}kg^{-1}{\cdot}d^{-1}$) and zoledronate (i.p. 100 $\mu g{\cdot}kg^{-1}{\cdot}d^{-1}$) (*D–F*) starting at P2. Vascular malformations of varying severity (*B*, *B′*, *C*, and *C′*) are significantly reduced in number following drug treatment (*E*, *E′*, *F*, and *F′*). (*A″–F″*) Representative images of flattened retinae isolated from wild-type and cKO littermates immunostained with PECAM (endothelial cells). Higher-magnification images of the boxed areas in *A″–F″* are shown at the right. Acute loss of CCM3 in endothelial cells results in lesioned areas with irregular vasculature (*B″* and *C″*) not seen in wild-type retina (*A″*). Drug treatment prevents abnormal development of retinal vasculature in cKO pups (*E″* and *F″*) without obvious effects on wild-type pups (*D″*). (*L* and *R*) Lesions on serial sagittal sections of hemicerebellum were processed with in situ hybridization for *Col4a1* to reveal the vasculature. (*S* and *T*) Lesions were classified in three groups, according to their diameter: small (<50 μm), medium (50–150 μm), and large (>150 μm) and were quantified ($n = 4$ pairs). Graphs indicate the number of small (*S*) and medium or large (*T*) lesions per hemicerebellum of vehicle- or drug-treated pups ($n = 4$ pairs). (*S*) Small, vehicle: 324.3 ± 63.78; drugs: 283.5 ± 59.97 (not significant). (*T*) Medium, vehicle: 74.25 ± 9.961; drugs: 38.75 ± 5.793 (*$P = 0.0216$); large, vehicle: 4.5 ± 1.555; drugs: 0.0 ± 0.0 (*$P = 0.0275$). See *SI Materials and Methods* for details. (*U*) Average radius of endothelial cell migration in flattened retinae of cKO neonates treated with vehicle or drugs ($n = 6$ pairs of untreated and treated retinae; *$P = 0.0069$, *t* test). (*V–X*) Kaplan–Meier survival curves. cKO neonates were induced with 35 mg/kg (*V* and *W*) or 10 mg/kg (*X*) tamoxifen at P1 (*V*) or P6 (*W* and *X*); treatment started 24 h after induction and continued to endpoint. Increase in lifespan in treated (P1: full dose: $n = 7$, $P = 0.0334$; P6: full dose: $n = 8$, $P = 0.0071$; low dose: $n = 6$, $P = 0.0734$; log-rank test) compared with untreated mice (P1, $n = 7$; P6, full dose, $n = 6$; low dose; $n = 5$). [Scale bars: 1 mm in *F* (applies to *A–F*) and *Q* (applies to *G–K* and *M–Q*); 0.5 mm in *F′* (applies to *A′–F′*) and *R* (applies to *L* and *R*); 200 μm in *F″* (applies to *A″–F″* low and high magnification.]

that fluvastatin (identified in an unbiased in vitro screen) and zoledronate, two FDA-approved drugs, reduce the severity of outcomes associated with CCM3 loss in primary astrocytes and reverse the effects of *ccm3* silencing in *Drosophila* glial cells in vivo. The drugs further reverse neural and vascular phenotypes in chronic and acute preclinical mouse models of CCM3 and significantly reduce lesion burden while extending longevity, suggesting that they are efficient in different cellular contexts. Importantly, both drugs cross the blood–brain barrier (https://www.drugbank.ca/), as also indicated by the results in this study. Our findings suggest that a two-step inhibition of the main trunk of the mevalonate pathway potently attenuates the effects of CCM3 loss and warrants studies to evaluate fluvastatin and zoledronate as a potential combined therapeutic intervention. Notably, familial CCM3 disease is associated with earliest onset and most severe prognosis, and its clinical phenotype is exceptionally aggressive (34). Our unbiased screen identified statins as the major candidate drug group for consideration in the context of CCM disease. Statins are well-studied and widely prescribed medicines. Fluvastatin, the first HMG-CoA reductase inhibitor to be synthetically prepared, has a short half-life with no active metabolites. In the clinical setting, it is used to treat dyslipidemias and as secondary prevention of cardiovascular disease. Exploring statins in the clinical population as therapy for CCM has proponents (35), despite potential

pathological outcomes associated with inhibition of prenylation (36). The results of a clinical trial to assess the effects of simvastatin on barrier permeability in *CCM1* patients are pending (ClinicalTrials.gov identifier: NCT01764451). Zoledronate, an inhibitor of farnesyl-pyrophosphate and geranyl-geranyl-pyrophosphate synthases, is approved to treat and prevent glucocorticoid-induced osteoporosis, hypercalcemia of malignancy, and multiple myeloma and bone metastases from solid tumors.

To date, various agents have been tested in preclinical models of CCM, including fasudil, which reduced lesion burden in *Ccm1* and *Ccm2* heterozygous mice (8), and simvastatin, which stabilized the endothelium of the latter (9) but failed to reduce lesion burden in mice lacking endothelial CCM2 (10), in contrast to cholecalciferol (vitamin D3) and tempol (a scavenger of superoxide) (10). Moreover, fasudil (but not simvastatin) reduced lesion burden and improved survival in sensitized *Ccm1* (but not *Ccm2*) heterozygous mice (11). The nonsteroidal antiinflammatory drug sulindac sulfide constrained vascular lesions in *Cdh5(PAC)CreERT2/Ccm3* cKO mice lacking endothelial CCM3 (28). Combined treatment with fluvastatin and zoledronate appears to have effects comparable to sulindac sulfide on survival; both approaches also reduced lesion burden, although slight differences in analyses preclude direct comparisons. Because endothelial gain of MEKK3 was suggested in CCM1 disease (33), future studies will likely test inhibitors of this cascade. In conclusion, fluvastatin/zoledronate combination therapy, which effectively inhibits the mevalonate pathway, warrants further evaluation as a pharmacological intervention in familial and potentially in sporadic CCM disease.

Materials and Methods

Animals. Mice were maintained in compliance with National Institutes of Health guidelines. Protocols were approved by the Yale University Institutional Animal Care and Use Committee. Details on mouse strains and drug administration are provided in *SI Materials and Methods*.

Cultures of Primary Astrocytes and Drug Screen. Primary astrocytes from wild-type and *hGfap/Ccm3* cKO littermates at P1 were isolated as previously described (5). The primary screening was performed at the Yale Center for Molecular Discovery.

The scratch-induced migration assay (37), analysis of retinal malformations (38), time-lapse microscopy (39), and lesion burden were performed as previously described. Details are provided in *SI Materials and Methods*.

Antibodies. The full list of antibodies used is reported in *SI Materials and Methods*.

ACKNOWLEDGMENTS. We thank Ralph Adams for sharing the *Cdh5(PAC)CreERT2* mice and Anne Eichmann for facilitating their transfer. This work was supported by NIH Grant NS046521 (to M.G.) and the Yale Program on Neurogenetics.

1. Russell DS, Rubenstein LJ (1989) *Pathology of Tumors of the Nervous System* (Williams and Wilkins, Baltimore).
2. Louvi A, Gunel M (2017) *Genetics of Cerebral Cavernous Malformations. Youmans and Winn Neurological Surgery*, ed Winn HR (Elsevier, Philadelphia), 7th Ed, pp 3547–3553.
3. Riant F, Bergametti F, Ayrignac X, Boulday G, Tournier-Lasserve E (2010) Recent insights into cerebral cavernous malformations: The molecular genetics of CCM. *FEBS J* 277:1070–1075.
4. Draheim KM, Fisher OS, Boggon TJ, Calderwood DA (2014) Cerebral cavernous malformation proteins at a glance. *J Cell Sci* 127:701–707.
5. Louvi A, et al. (2011) Loss of cerebral cavernous malformation 3 (Ccm3) in neuroglia leads to CCM and vascular pathology. *Proc Natl Acad Sci USA* 108:3737–3742.
6. Louvi A, Nishimura S, Günel M (2014) Ccm3, a gene associated with cerebral cavernous malformations, is required for neuronal migration. *Development* 141: 1404–1415.
7. Stockton RA, Shenkar R, Awad IA, Ginsberg MH (2010) Cerebral cavernous malformations proteins inhibit Rho kinase to stabilize vascular integrity. *J Exp Med* 207: 881–896.
8. McDonald DA, et al. (2012) Fasudil decreases lesion burden in a murine model of cerebral cavernous malformation disease. *Stroke* 43:571–574.
9. Whitehead KJ, et al. (2009) The cerebral cavernous malformation signaling pathway promotes vascular integrity via Rho GTPases. *Nat Med* 15:177–184.
10. Gibson CC, et al. (2015) Strategy for identifying repurposed drugs for the treatment of cerebral cavernous malformation. *Circulation* 131:289–299.
11. Shenkar R, et al. (2017) RhoA kinase inhibition with fasudil versus simvastatin in murine models of cerebral cavernous malformations. *Stroke* 48:187–194.
12. Zhang FL, Casey PJ (1996) Protein prenylation: Molecular mechanisms and functional consequences. *Annu Rev Biochem* 65:241–269.
13. Elsayed M, et al. (2016) Synergistic antiproliferative effects of zoledronic acid and fluvastatin on human pancreatic cancer cell lines: An in vitro study. *Biol Pharm Bull* 39: 1238–1246.
14. Varela I, et al. (2008) Combined treatment with statins and aminobisphosphonates extends longevity in a mouse model of human premature aging. *Nat Med* 14:767–772.
15. Yuasa T, Kimura S, Ashihara E, Habuchi T, Maekawa T (2007) Zoledronic acid - a multiplicity of anti-cancer action. *Curr Med Chem* 14:2126–2135.
16. Caraglia M, et al. (2010) Zoledronic acid: An unending tale for an antiresorptive agent. *Expert Opin Pharmacother* 11:141–154.
17. Walter C, Pabst A, Ziebart T, Klein M, Al-Nawas B (2011) Bisphosphonates affect migration ability and cell viability of HUVEC, fibroblasts and osteoblasts in vitro. *Oral Dis* 17:194–199.
18. McLeod NM, Moutasim KA, Brennan PA, Thomas G, Jenei V (2014) In vitro effect of bisphosphonates on oral keratinocytes and fibroblasts. *J Oral Maxillofac Surg* 72: 503–509.
19. Argaw AT, et al. (2006) IL-1beta regulates blood-brain barrier permeability via reactivation of the hypoxia-angiogenesis program. *J Immunol* 177:5574–5584.
20. Goudreault M, et al. (2009) A PP2A phosphatase high density interaction network identifies a novel striatin-interacting phosphatase and kinase complex linked to the cerebral cavernous malformation 3 (CCM3) protein. *Mol Cell Proteomics* 8:157–171.
21. Song Y, Eng M, Ghabrial AS (2013) Focal defects in single-celled tubes mutant for Cerebral cavernous malformation 3, GCKIII, or NSF2. *Dev Cell* 25:507–519.
22. Fruttiger M (2007) Development of the retinal vasculature. *Angiogenesis* 10:77–88.
23. Vintonenko N, et al. (2012) Transcriptome analysis and in vivo activity of fluvastatin versus zoledronic acid in a murine breast cancer metastasis model. *Mol Pharmacol* 82: 521–528.
24. Hayashidani S, et al. (2002) Fluvastatin, a 3-hydroxy-3-methylglutaryl coenzyme a reductase inhibitor, attenuates left ventricular remodeling and failure after experimental myocardial infarction. *Circulation* 105:868–873.
25. Zadelaar S, et al. (2007) Mouse models for atherosclerosis and pharmaceutical modifiers. *Arterioscler Thromb Vasc Biol* 27:1706–1721.
26. Cahoy JD, et al. (2008) A transcriptome database for astrocytes, neurons, and oligodendrocytes: A new resource for understanding brain development and function. *J Neurosci* 28:264–278.
27. Boulday G, et al. (2011) Developmental timing of CCM2 loss influences cerebral cavernous malformations in mice. *J Exp Med* 208:1835–1847.
28. Bravi L, et al. (2015) Sulindac metabolites decrease cerebrovascular malformations in CCM3-knockout mice. *Proc Natl Acad Sci USA* 112:8421–8426.
29. Maddaluno L, et al. (2013) EndMT contributes to the onset and progression of cerebral cavernous malformations. *Nature* 498:492–496.
30. Renz M, et al. (2015) Regulation of β1 integrin-Klf2-mediated angiogenesis by CCM proteins. *Dev Cell* 32:181–190.
31. Zhou Z, et al. (2015) The cerebral cavernous malformation pathway controls cardiac development via regulation of endocardial MEKK3 signaling and KLF expression. *Dev Cell* 32:168–180.
32. Cuttano R, et al. (2016) KLF4 is a key determinant in the development and progression of cerebral cavernous malformations. *EMBO Mol Med* 8:6–24.
33. Zhou Z, et al. (2016) Cerebral cavernous malformations arise from endothelial gain of MEKK3-KLF2/4 signalling. *Nature* 532:122–126.
34. Shenkar R, et al. (2015) Exceptional aggressiveness of cerebral cavernous malformation disease associated with PDCD10 mutations. *Genetics Med* 17:188–196.
35. Li DY, Whitehead KJ (2010) Evaluating strategies for the treatment of cerebral cavernous malformations. *Stroke* 41(10, Suppl):S92–S94.
36. Eisa-Beygi S, Wen XY, Macdonald RL (2014) A call for rigorous study of statins in resolution of cerebral cavernous malformation pathology. *Stroke* 45:1859–1861.
37. Etienne-Manneville S (2006) In vitro assay of primary astrocyte migration as a tool to study Rho GTPase function in cell polarization. *Methods Enzymol* 406:565–578.
38. Tual-Chalot S, Allinson KR, Fruttiger M, Arthur HM (2013) Whole mount immunofluorescent staining of the neonatal mouse retina to investigate angiogenesis in vivo. *J Vis Exp* 77:e50546.
39. Smith CL, et al. (2016) Migration phenotype of brain-cancer cells predicts patient outcomes. *Cell Reports* 15:2616–2624.
40. Wang Y, et al. (2010) Ephrin-B2 controls VEGF-induced angiogenesis and lymphangiogenesis. *Nature* 465:483–486.
41. Poujade M, et al. (2007) Collective migration of an epithelial monolayer in response to a model wound. *Proc Natl Acad Sci USA* 104:15988–15993.
42. Holden P, Horton WA (2009) Crude subcellular fractionation of cultured mammalian cell lines. *BMC Res Notes* 2:243.